CITE AS *Frankl, A., Stal, C., Abraha, A., Nyssen, J., Rieke-Zapp, D., De Wulf, A., Poesen, J., 2015. Detailed recording of gully morphology in 3D through image-based modelling. Catena 127, 92-101.*

Detailed recording of gully morphology in 3D through image-based modelling

Amaury Frankl[1,a,*], Cornelis Stal[1,a], Amanuel Abraha[2], Jan Nyssen[1], Dirk Rieke-Zapp [3], Alain De Wulf [1], Jean Poesen [4]

[a] Both authors contributed equally to this work.

[1] Department of Geography, Ghent University, Belgium.

[2] Institute of Climate and Society, Mekelle University, Ethiopia.

[3] Breuckmann GmbH, D-88709 Meersburg, Germany.

[4] Division of Geography, Department of Earth and Environmental Sciences, KU Leuven, Belgium.

* Corresponding author: Tel.: +32 92644701; fax: +32 92644985; e-mail address: amaury.frankl@ugent.be (A. Frankl)

Abstract

The ability to understand gully erosion development is closely related to our ability to quantify the morphology of gullies. At present, various technologies are at hand to collect data at increasing levels of detail. However, many of the developed technologies are time-consuming, difficult to apply or expensive. As an alternative, image-based modelling offers a cost-efficient, flexible and rapid method to quantify gully morphology from photographs taken in the field. In this study, the use of image-based modelling was tested and fine-tuned to quantify the

CITE AS *Frankl, A., Stal, C., Abraha, A., Nyssen, J., Rieke-Zapp, D., De Wulf, A., Poesen, J., 2015. Detailed recording of gully morphology in 3D through image-based modelling. Catena 127, 92-101.*

morphology of four gully heads in contrasting biophysical environments prone to gully erosion: two bank gullies in Central Belgium and two permanent gullies in Northern Ethiopia. Ground photographs (n = 88-235) were taken with a reflex Canon EOS 450D camera having a 20 mm wide-angle lens with a fixed focal length. The data collection occurred during days of 30-100% cloud cover and after removing excessive vegetation in the gullies. Processing of the photographs occurred in PhotoScan 1.0.2. software using the semi-automated Structure from Motion-Multi View Stereo (SfM-MVS) workflow, and allowed to produce 3D Digital Elevation Models with accuracies that range from millimetres to centimetres. In addition, for the same surface, 2.5D models were created in ArcGIS. Gully morphological properties were derived and include cross-sections, total volume and volume of undercut walls and soil pipe inlets. For the volume calculation, OPTOCAT software was used. Cross-sections were also quantified by tape meter measurements. When compared to 3D models, cross-sections quantified from tape meter measurements and from 2.5D models underestimate the cross-sectional area by <1-14% and 0-2.5% respectively. Considering gully volume, 2.5D and 3D approximations show only small differences, related to the volume of soil pipe inlets and undercutting areas. These differences, however, highlight the erosive activity of the gullies, and are important to understand gully dynamics in detail. Geomorphologically spoken, areas where undercutting or soil piping occurs are among the most dynamic and reveal where important morphologic changes are about to occur. The accuracies reported in this study are similar to those obtained in other studies that consider surfaces of similar scales. In sum, image based modelling is a promising tool to study in detail gully morphology in 3D, which is the closest approximation of the surface morphology.

CITE AS *Frankl, A., Stal, C., Abraha, A., Nyssen, J., Rieke-Zapp, D., De Wulf, A., Poesen, J., 2015. Detailed recording of gully morphology in 3D through image-based modelling. Catena 127, 92-101.*

Keywords: PhotoScan; Digital Elevation Model (DEM); soil pipes; Structure from Motion-Multi View Stereo (SfM-MVS); volume calculation.

1. Introduction

Detailed understanding of the causes and consequences of soil erosion is of paramount importance whenever societies want to ensure their sustainability, especially facing global climate change (Montanarella and Vargas, 2012). Thoughtless planning has frequently shown that the delicate balance between the exploitation of natural resources and the resilience of the environment can easily be violated. Deforestation, agricultural intensification, overgrazing, urbanization and flow diversion by infrastructure construction are frequently mentioned as causes of accelerated erosion by gullying and river channel degradation (Knighton, 1998; Schumm, 2005). Typical for dryland environments is severe gully erosion and river channel degradation related to the degradation of the vegetation cover and flow diversions, often in combination with the occurrence of climatic shocks (Valentin *et al.*, 2005). In subhumid and humid environments, rapid gully development and river bed degradation also occurs when poor land management is applied. Most striking in that regard is probably the incision of tropical soils after the clearance of rain forests (e.g., Clarke and Walsh, 2006). In light of striving towards a 'land-degradation neutral' world, a Rio+20 conference target, rapid and detailed understanding of local erosion processes is ever more crucial. This requires scientists to rapidly access precise data on the development of erosion features, so that causal relations can be thoroughly understood.

CITE AS *Frankl, A., Stal, C., Abraha, A., Nyssen, J., Rieke-Zapp, D., De Wulf, A., Poesen, J., 2015. Detailed recording of gully morphology in 3D through image-based modelling. Catena 127, 92-101.*

Methods for monitoring morphological changes of gullies and river channels are mostly based on in-situ measuring techniques or quantifications from remote sensing products and their Digital Elevation Model (DEM) derivates (Poesen *et al.*, 2003). In situ measuring is often time consuming and requires accurate measuring equipment, like a total station, highly accurate Global Navigation Satellite System (GNSS) receivers, or laser profilometers (Castillo *et al*., 2012), which are not always at hand or are expensive to rent. Moreover, very dense measurements of xyz-coordinates are usually required to fully grasp the morphological developments in channel degradation or aggradation. This is only offered by the use of Terrestrial Laser Scanning (TLS) (Perroy *et al.*, 2012) or Airborne Laser Scanning (ALS) (Heritage and Hetherington, 2007). The use of TLS is limited for the same reasons as for the conventional topographic sensors. ALS often lacks the accuracy to precisely capture the morphology of small channels (Perroy *et al.*, 2010), and in terms of cost and feasibility, its use is also limited for most monitoring projects. Other remote sensing products, such as aerial photographs and satellite images, need to have a sufficiently high resolution to accurately quantify volumes from their DEM products (Giménez *et al.*, 2009). High resolution images (having a resolution <1 m) are increasingly available at short time intervals. However, when requiring stereoscopic views, acquiring the images is usually financially out of reach of most projects. Collecting high resolution data is also done from a remotely controlled blimp from which large-scale stereographic aerial photographs can be taken (Ries and Marzolff, 2003; Marzolff and Poesen 2009). Similar data can be obtained from cameras which are mounted on Unmanned Aerial Vehicles (UAVs). Given their low-cost and flexible nature, the latter are

increasingly being used in geosciences applications (Corbane *et al.*, 2008; Hendrickx *et al.*, 2011; Lucieer *et al.*, 2013; Peter *et al.*, 2014). Image-based modelling is a recent and promising development in photogrammetry which allows to created textured models from a set of conventional terrestrial or airborne photographs, taken from the same surface. The methodology is based on semi-automated Structure from Motion and MultiView Stereo (SfM-MVS) workflows (Seitz *et al.*, 2006; Verhoeven *et al.*, 2013; Javernick *et al.*, 2014), which are integrated in software such as PhotoScan (Agisoft). It is rapidly gaining interest of various scientific disciplines which require to model objects or terrain features, often in combination with UAV surveys. For example, image-based modelling was used to produce accurate models of historical globes (Stal *et al.*, 2012), buildings (Stal *et al.* 2011), gullies (Castillo *et al.*, 2012; Gómez-Gutiérrez *et al.*, 2014; Kaiser *et al.*, 2014), landforms (James and Robson, 2012) and even specific landscapes (Verhoeven *et al.*, 2012). However, most studies use image-based modelling in a 2.5D environment, in which every xy-coordinate yields only one z-coordinate. This is often related to the nature of recording from an airborne perspective (e.g., aerial photography), from which vertical morphologies are (largely) hidden from the observation point (Giménez *et al.*, 2009; Marzolff and Poesen, 2009). For erosion studies, understanding in detail the erosion dynamics and processes involved, however, requires to produce 3D models, in which the actual 3D topography is approximated, including areas for which multiple z-coordinates exist for unique xy-coordinates. This allows to model complex morphologies such as soil pipe inlets and overhanging walls, which are key indicators of the erosivity of the gully headcut (Frankl *et al.*, 2012).

CITE AS *Frankl, A., Stal, C., Abraha, A., Nyssen, J., Rieke-Zapp, D., De Wulf, A., Poesen, J., 2015. Detailed recording of gully morphology in 3D through image-based modelling. Catena 127, 92-101.*

Therefore, the objective of this study is to present the use of image-based modelling for the production of detailed 3D models of gully heads from a ground-based approach. The method allows better understanding of gully morphologies, required to understand processes involved, and can be used to monitor changes at very high spatio-temporal scales.

2. Material and methods

2.1 Selected sites

The study areas represent two contrasting environments sensitive to gully erosion, i.e. the rolling landscape of the European loess belt (Poesen and Govers, 1990) and the east African highlands (Frankl *et al.*, 2011, 2012; Fig. 1). Two bank gullies were selected in Bertem, located in the Belgian loess belt (Bel1: 50.833°N, 4.630°E and Bel 2: 50.837°N, 4.621°E; Fig. 2), where elevations range between 20 and 110 m a.s.l. The selected gullies developed in sunken lane banks, representing an important cause of soil losses in the region (Poesen et al. 1996). Gully Bel2 was partially filled soon after data collection by a farmer in order to limit the loss of agricultural land by the rapid expanding gully head.

The lithology consists of unconsolidated Cenozoïc marine sands covered by a loess layer with a thickness varying between a few decimetres up to several meters (Vanwalleghem *et al.*, 2005). Typical soils for these deposits are Haplic Luvisols with a clay-illuviation horizon (Bt) at 35-45 cm below the soil surface (Vanwalleghem *et al.*, 2005). According to the Köppen-Geiger climate classification, this area is characterized by a Cfb humid temperate climate with no dry season and warm summers (Peel *et al.*, 2007). Annual precipitation varies between 750 to 800 mm y^{-1}

CITE AS *Frankl, A., Stal, C., Abraha, A., Nyssen, J., Rieke-Zapp, D., De Wulf, A., Poesen, J., 2015. Detailed recording of gully morphology in 3D through image-based modelling. Catena 127, 92-101.*

(Alexandre *et al.*, 1998). Another two gully heads were selected in Adi Kwolakol (near Hagere Selam), located in the north Ethiopian highlands (Eth1: 13.655°N, 39.209°E and Eth2: 13.654°N, 39.210°E; Fig. 2), where elevations range between 2000 and 4500 m a.s.l. Here, Mesozoïc sandstones and limestones, and Cenozoïc basalts are exposed (Merla *et al.*, 1979). Due to intense geomorphological processes, Regosols, Cambisols and Leptosols dominate the soil catenas that developed on the different lithologies (Nyssen *et al.*, 2008). The climate is classified as hot semiarid Bsh, with a prolonged dry season and a short monsoon-type rainy season (Peel *et al.*, 2007). Annual precipitation shows a large inter-annual variability and is on average 550 mm y^{-1} (Jacob *et al.*, 2013).

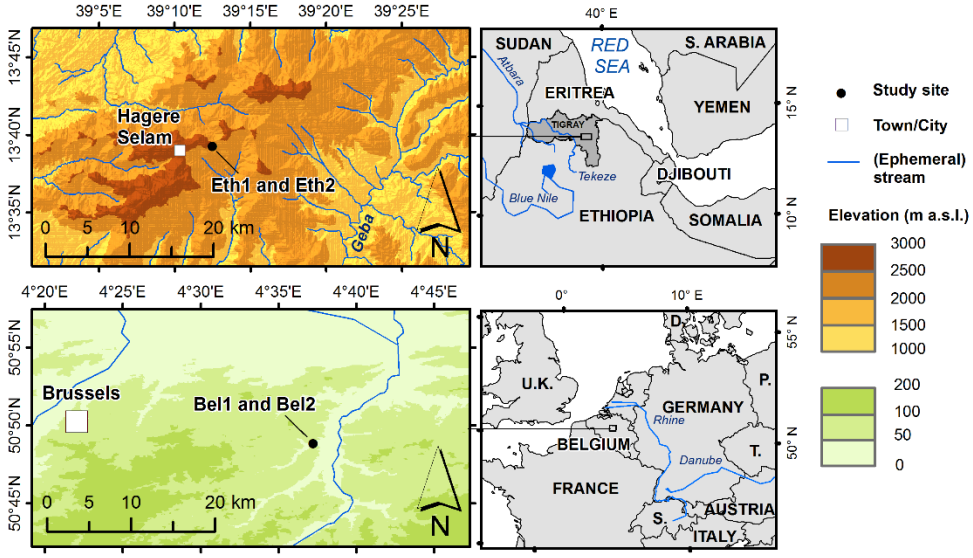

Figure 1: Location of study sites in Belgium and Ethiopia.

CITE AS *Frankl, A., Stal, C., Abraha, A., Nyssen, J., Rieke-Zapp, D., De Wulf, A., Poesen, J., 2015. Detailed recording of gully morphology in 3D through image-based modelling. Catena 127, 92-101.*

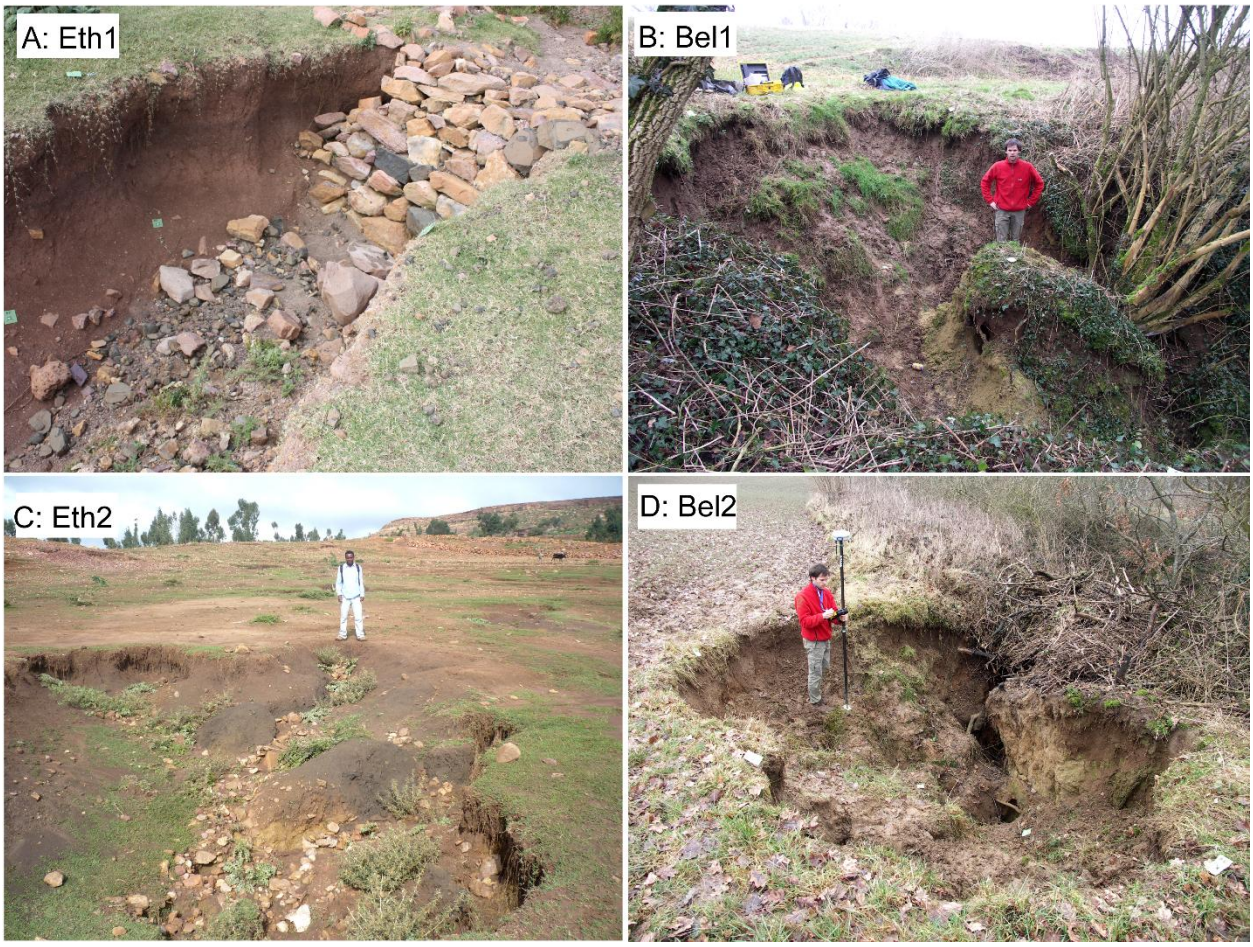

Figure 2: Selected gully heads in Ethiopia (A,C) and in Belgium (B,D) used for image-based 3D modelling.

2.2 Data collection

Data collection occurred on February 21, 2013 in Belgium (gullies Bel1 and Bel2) and on June 12, 2013 in Ethiopia (gullies Eth1 and Eth2). Inside the gullies, where necessary, vegetation was clipped near the soil surface. This was especially required for the gullies in Belgium where tall grass grew on the gully walls and bottom, and some large shrubs overgrew the gullies. Markers

were installed at the gully headcuts in order to indicate both Ground Control Points (GCPs) and gully cross-sections. For each gully head, one or two cross-sections were defined by marking the profile knick points along a vertical plane. Cross-sections top width, bottom width and maximum depth (m) were quantified using a tape meter. As a high-accuracy Trimble R6 GNSS antenna (using the Flemish Real Time Kinematic network, FLEPOS) was available for the measurements in Belgium, 20 GCPs were recorded for gullies Bel1 and Bel2 (Fig. 2D), and 103 randomly distributed measurements were done for an accuracy assessment. Planimetric and altimetric accuracies of these measurements were between 3 and 6 cm (95% or 2 standard deviations; AGIV, 2008). For the measurements in Ethiopia, an accurate GNSS was not available, neither in RTK, nor in differential mode. Therefore, a handheld Garmin Etrex GPS (2 m standard deviation) was used to record one GCP for the gullies Eth1 and Eth2. For the scaling and referencing of Eth1 and Eth2 (Section 2.3), the distance between two to three GCPs was measured in the field. Moreover, the orientation between the GCP used for positioning the model and nearby GCPs was measured by compass.

Photographic recording of the gully heads was done when there was no direct irradiance from the sun in the gullies. The latter would produce cast shadows, causing large differences in contrast between light and dark areas, making image matching in the image modelling (Section 2.3) less accurate or potentially impossible. Collecting photographs for the production of virtual 3D models was done with a reflex Canon EOS 450D camera, having a 20 mm wide-angle lens and a fixed focal length (35 mm equivalent focal length is 28.6 mm). No special camera settings were required, only those that ensure sharp images having good contrast given the light

conditions without the need of using the flash. Photographing the gully headcuts was done from several viewpoints (located both outside and inside the gully), thus creating a large dataset of overlapping photographs (Fig. 3). By recording from multiple viewpoints with approximately parallel baselines, and by respecting a minimum overlap of 50% between subsequent photographs, parallaxes needed for the 3D modelling were created. Gully Bel2 that was filled by farmer operations was rephotographed in order to have both the incised and the filled situation for that gully.

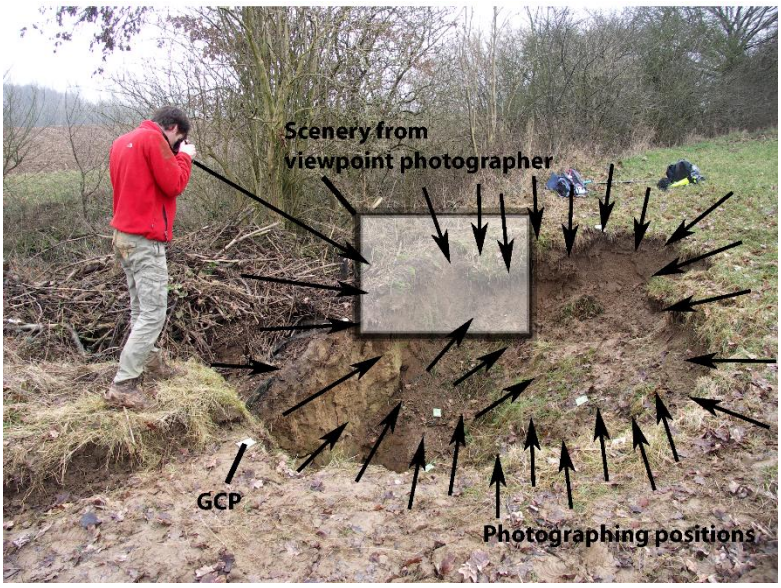

Figure 3: Data acquisition (at bank gully head Bel2) occurs by photographing the gully head from multiple viewpoints (including from inside the gully), ensuring 50% overlap between subsequent recordings. A fixed zoom is chosen in relation to the scenery covered from the viewpoints. Arrows indicate direction of photographs taken.

CITE AS *Frankl, A., Stal, C., Abraha, A., Nyssen, J., Rieke-Zapp, D., De Wulf, A., Poesen, J., 2015. Detailed recording of gully morphology in 3D through image-based modelling. Catena 127, 92-101.*

2.3 Image-based 3D modelling and accuracy assessment

Producing virtual 3D models from the photographs was based on a Structure from Motion – Multi-View Stereo (SfM-MVS) integrated workflow (Fig. 4). It is implemented in various software, such as Blender, Microsoft PhotoSynth or PhotoScan (version 1.0.2., Agisoft), with the latter being used here. The whole procedure runs automatically, only requiring the photographs and their metadata from the EXIF image-files (like focal length, focal point and image size) as inputs. If metric 3D models are required, the workflow will be semi-automatic, as GCPs need to be identified manually. Furthermore, user-interference is required for quality control and for the (optional) manual edition and fine-tuning of the models (delete peaks and troughs which result from erroneous matching). The SfM-MVS methodology is very similar to conventional photogammetry, with the main difference that instead of using one stereo couple, a large series of photographs of the same scene is used. Basically, the SfM method allows to create a 3D structure from multiple 2D images (i.e. terrestrial photographs). This included a feature point detection and description, image matching (cfr., defining tie-points), image triangulation and bundle adjustment (creation of a sparse 3D point cloud of image matching points based on the projection of image pixels in 3D).

Referencing the 3D models into a coordinate system was done in a different way for the gully heads in Belgium and those in Ethiopia. For the gullies Bel1 and Bel2 (and $Bel2_{Filled}$), 20 GCPs (measured with Trimble R6 GNSS antenna) were used to scale and georeference the 3D models into the UTM-WGS1984 coordinate system. For the gullies Eth1 and Eth2, the 3D models were first scaled using the measured distance between two to three GCPs (Section 2.2). As these

205 measurements occurred with a tape meter, accurate at centimetre-level, the relative accuracy is
206 ought to be similar to the georeferencing of the Bel1 and Bel2 gullies. Positioning the gully
207 models Eth1 and Eth2 in the UTM-WGS 1984 coordinate system was done using one GCP
208 (measured with handheld GPS). Resolving the tilt in X, Y and Z was done by considering the
209 orientation between the GCP used for positioning the model and nearby GCPs, and by
210 considering a vertical plane defined along the cross-sections.
211 Resolving the 3D geometry was done with the MVS method (in PhotoScan 1.0.2.), allowing
212 producing a dense estimate of the surface geometry in the form of a Triangulated Irregular
213 Network (TIN). This is based on the intersection of corresponding pixels projected from different
214 camera positions and orientations in 3D (Lourakis and Argyros, 2009). The triangulation of the
215 mesh occurred by connecting all points in the 3D model (Pfeifer, 2002). In order to quantify the
216 importance of soil piping and undercutting at the gully head, an additional 2.5D models from the
217 triangulated mesh was created in ArcGIS 10 (ESRI).
218

CITE AS *Frankl, A., Stal, C., Abraha, A., Nyssen, J., Rieke-Zapp, D., De Wulf, A., Poesen, J., 2015. Detailed recording of gully morphology in 3D through image-based modelling. Catena 127, 92-101.*

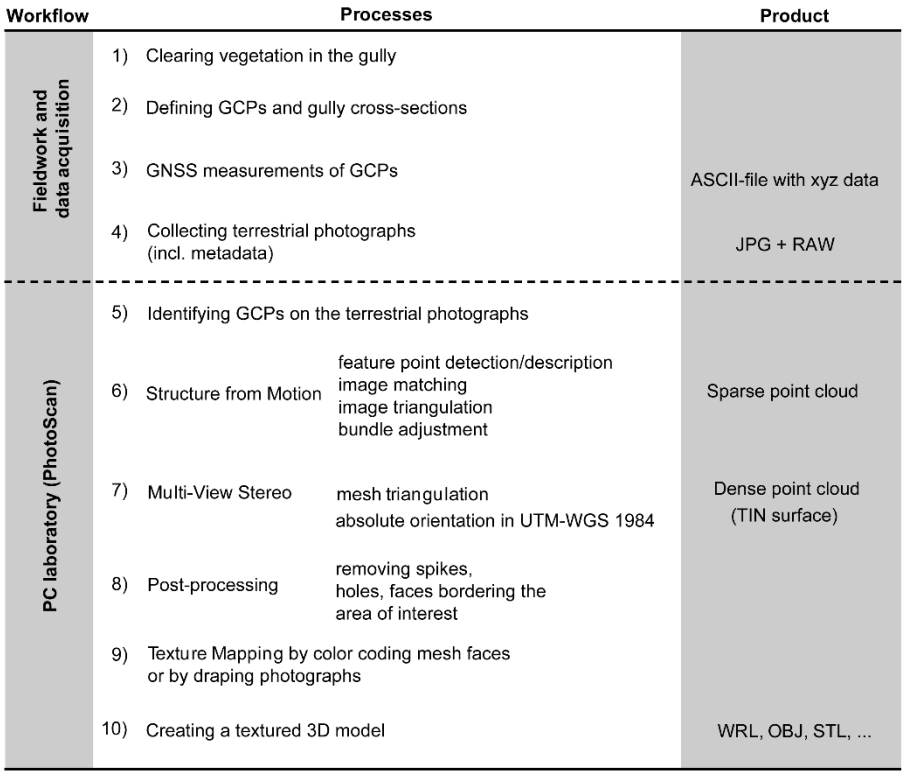

Figure 4: The major steps in image-based 3D modelling. The implementation of this scheme in PhotoScan can be found on http://www.agisoft.ru/.

During the geometric 3D reconstruction, a single colour value, based on averaged colour values of all corresponding pixels from different images, was assigned to each face in the mesh. A detailed and photorealistic texture map was obtained by projecting photographs onto the mesh. Full description of the SfM-MVS methodology and image-based 3D modelling can be found in Robertson and Cipolla (2009), Seitz *et al.* (2006) and Remondino and El-Hakim (2006).

The overall accuracy of the models was assessed by comparing distances between GCP measured in the field (not used in the DEM creation) with those computed from the 3D models.

CITE AS *Frankl, A., Stal, C., Abraha, A., Nyssen, J., Rieke-Zapp, D., De Wulf, A., Poesen, J., 2015. Detailed recording of gully morphology in 3D through image-based modelling. Catena 127, 92-101.*

In addition, for the Bel1 and Bel2 models, the elevation of extra GNSS sample points were compared to the elevation of the corresponding planimetric position in the 3D model. The resulting RMSE in z allowed assessing the accuracy of the 3D models, in relation with the accuracy of the GNSS measurements.

2.4 Analysing gully morphology and volumes

First, a visual analysis of the draped 3D models was performed. Second, cross-sections that were measured in the field were compared to those derived from the 2.5D and 3D models. From field measurements, cross-sectional area is typically described by the formula:

$$CSA = ((TW+BW)/2)*D \quad \text{(eq. 1)}$$

With CSA= cross-sectional area (m^2), TW= top width (m), BW= bottom width (m) and D= maximum depth (m). Cross-sections from the 2.5D models were created with Spatial Analyst in ArcGIS10. For the 3D models, Spark (Geomagic) was used.

For the calculation of 2.5D and 3D volumes, the models were imported in STL format into OPTOCAT 2014 software (Breuckmann 2014 – http://www.breuckmann.com). Since volume calculations require a closed mesh and the PhotoScan mesh output contained many flipped triangles and holes, the OPTOCAT´s hole fill module was used to improve the mesh. Afterwards an inclined plane was fitted around the gully outline to determine the upper limit of the volume calculation and to calculate 3D and 2.5D volumes. The 2.5D representation was calculated from

the 3D data with OPTOCAT´s analysis tools. The raster resolution was chosen to represent 10 mm in reality, i.e. a regular X,Y- raster with sampling distance of 10 mm. The 2.5D model could be calculated representing the minimum, maximum or average projected height in the given X, Y cell. In this case the maximum height was chosen to calculate the difference between 3D and 2.5D volumes. Calculation of the volume under the reference plane for the 3D and 2.5D surfaces was performed using OPTOCAT´s calculate volume function.

3. Results

The image-based 3D models of the gullies were produced based on 88 up to 235 photographs (Table 1). The Ground Sampling Distance (GSD), which is a measure for the model-resolution in xyz, varied between 0.45 mm and 0.72 mm. The relative accuracy of the models was expressed by comparing distances between GCPs measured in the field (ranging from ca. 0.5 to 3 m), to those computed from the models. For gullies Bel1 and Bel2 and Eth1, this error was very small, at millimeter to centimeter level (Table 1). This coincides to a weighted average error smaller than 1%. For gully Eth2, the accuracy error of the model was one order of magnitude larger, with the distance error being 0.1 m and the weighted average 9%. The latter can however largely be explained by an outlier in the dataset (possible a spike in the model), as can also be derived from the much smaller standard deviation. As GNSS measurements were available for Bel1 and Bel2, an $RMSE_z$ was computed on a large set of points. The resulting errors were 0.148 m for Bel1 and 0.155 m for Bel2, which is similar to the 0.05-0.10 m accuracy level of the GNSS measurements (Table 1). Note that the rather low accuracy of the GNSS sensor was caused by a limited number

of satellite signals received by the antenna while measuring under/in the proximity of trees.

Table 1: 3D Models characteristics and accuracies.

DEM	No. of photographs	Recording distance (m)	GSD (m)	Error on measured distances in field vs model (m)				RMSE	
				n	average (m)	st.dev. (m)	weighted average (%)	n	z (m)
Bel1	235	ca. 1-6 m	0.00048	11	0.007	0.190	0.5	53	0.148
Bel2	180	ca. 1-5 m	0.00072	8	0.010	0.017	0.5	63	0.155
Eth1	140	ca. 2-7 m	0.00045	17	0.007	0.011	0.5	x	x
Eth2	88	ca. 1-5 m	0.00048	14	0.109*	0.046	9.0	x	x

*high value linked to an outlier

Fig. 5A-D shows both the 2.5D and the image-based 3D models of gully Bel1 and Eth1. The 2.5D models show the gully morphology from a vertical perspective, in a conventional representation of a shaded colour-coded elevation range. Visual analysis of these models reveal the details of the gully morphology, including vertical walls and large soil clods and boulders on the floor of gully Eth1, and for Bel1, a closed depression (<0.5 m) on the gully floor. 3D visualizations of these models would not give us more information on the gully morphology, as each xy-coordinate has only one z-coordinate. Similar views are given for the 3D photomodels, that were colour coded by using the average pixel colour values of photographs used to create the surface. As can be observed in Fig. 7, 3D visualisations do provide additional information, as overhanging walls and pipe inlets become visible. This is related to the possibility to assign multiple z-coordinates to single xy-coordinates in the 3D models.

CITE AS *Frankl, A., Stal, C., Abraha, A., Nyssen, J., Rieke-Zapp, D., De Wulf, A., Poesen, J., 2015. Detailed recording of gully morphology in 3D through image-based modelling. Catena 127, 92-101.*

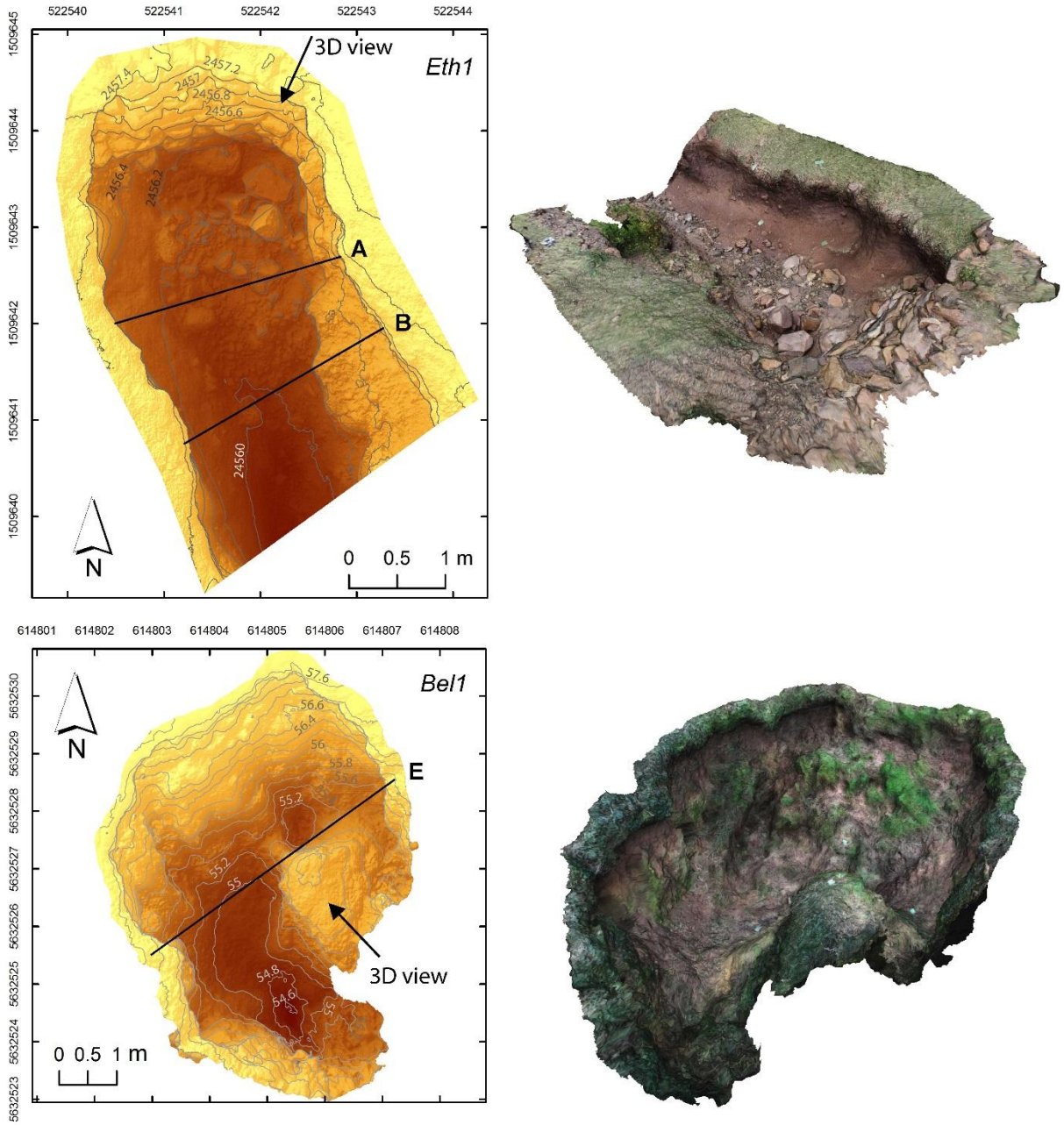

287

288 **Figure 5**: Examples of 2.5D DEMs of gullies Eth1 and Bel1 (left) and the respective draped 3D
289 photomodels (from an oblique viewpoint). Cross-sectional profiles are given in Fig. 6.

CITE AS *Frankl, A., Stal, C., Abraha, A., Nyssen, J., Rieke-Zapp, D., De Wulf, A., Poesen, J., 2015. Detailed recording of gully morphology in 3D through image-based modelling. Catena 127, 92-101.*

290 Coordinates are in UTM-WGS1984.

291

292 Considering the gully cross-sectional profiles, a comparison was made between the cross-
293 sections as measured in the field to those derived from the 2.5D and 3D models. Simple
294 approximation of cross-sections in the field by equation 1 can yield relatively good results, with
295 differences of <1% up to 14% when compared to the cross-sections computed from the image-
296 based 3D models (Table 2). However, to understand gully erosion dynamics, the cross-sections
297 derived from the image-based 3D models are much more informative. From the cross-sections
298 alone, we can derive that gully head Eth1 is more erosive than Eth2, the former having steep
299 undercut walls and the latter having smooth and gently sloping walls (Fig. 6A-F). Moreover, a
300 stabilization level can be observed on the gully floor of Eth1, corresponding to a previous
301 equilibrium status (Fig. 6B). Similar observations can be made on the cross-sections of gullies
302 Bel1 and Bel2. Both have undercut walls, which on cross-section E connects to a soil pipe (Fig.
303 6E). A comparison of the cross-sectional areas computed from the 2.5D models with the 3D
304 models shows that the former slightly underestimate (up to 2.5%) the gully cross-sectional area,
305 as the 2.5D models not include the undercut gully walls (Table 2).

306

Table 2: Gully cross-sections and volumes.

Gully	Cross-section	Cross-sectional area (m^2)			Difference %	
		Tape meter	Model 2.5D	Model 3D	Field-M3D	M2.5D-M3D
Eth1	A	2.33	2.24	2.29	1.7	-2.2
Eth1	B	2.91	2.61	2.68	8.6	-2.6
Eth2	C	0.99	1.01	1.01	-2.0	0

Eth2	D	0.81	0.71	0.71	14.1	0
Bel1	E	8.56	8.33	8.54	0.2	-2.5
Bel2	F	7.51	7.06	7.11	5.6	-0.7

	Volume (m³)		**Difference**	
Gully	Model 2.5D	Model 3D	M2.5D-M3D (%)	M2.5D-M3D (m³)
Bel1	29.08	29.27	-0.65	-0.19
Bel2	18.99	19.26	-1.4	-0.27
Eth1	18.12	18.18	-0.33	-0.06
Eth2	2.17	2.17	0	0

307

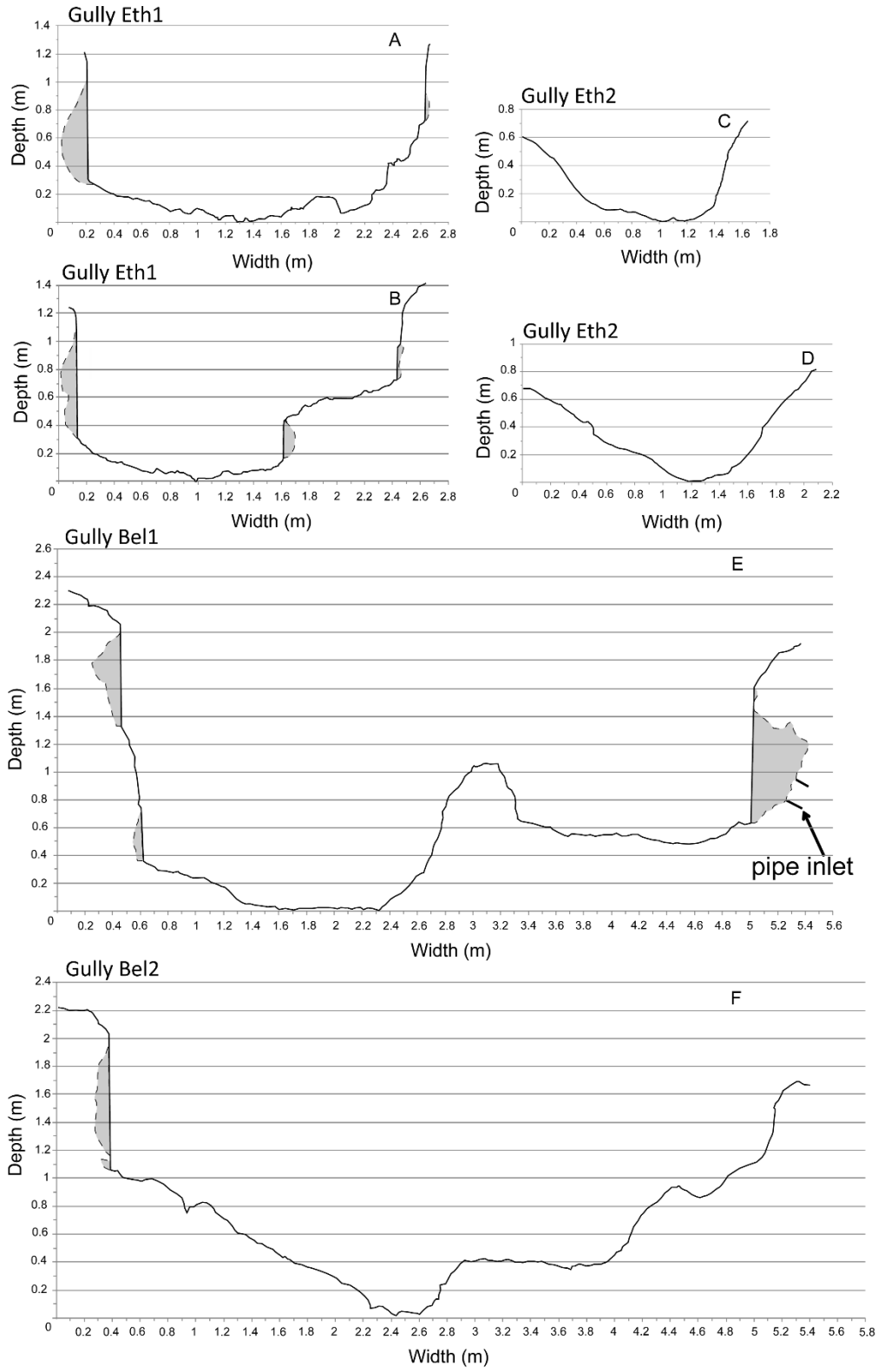
Gully Eth1
A
Depth (m)
Width (m)
Gully Eth2
C
Depth (m)
Width (m)
Gully Eth1
B
Depth (m)
Width (m)
Gully Eth2
D
Depth (m)
Width (m)
Gully Bel1
E
pipe inlet
Depth (m)
Width (m)
Gully Bel2
F
Depth (m)
Width (m)

CITE AS *Frankl, A., Stal, C., Abraha, A., Nyssen, J., Rieke-Zapp, D., De Wulf, A., Poesen, J., 2015. Detailed recording of gully morphology in 3D through image-based modelling. Catena 127, 92-101.*

309 **Figure 6**: The cross-sectional profiles derived from 2.5D models show vertical walls when
310 undercutting occurs (black lines). These undercut gully walls (grey fill on cross-section) do occur
311 on the 3D models prepared from image-based 3D modelling. All sections are at the same scale
312 and with no vertical exaggeration.
313
314 The gully volume calculations in 2.5D and 3D are given in Table 2, and the differences between
315 the two model types range between 0 and 0.27 m^3. Although these values are rather small,
316 especially compared with the total volume of the headcuts, these values represent the volume of
317 the undercuts and pipe inlets, and thus, are indicators of the erosive activity of the gully. The
318 incised Bel2 and $Bel2_{Filled}$ models were combined in Fig. 7 and thus represent the volume of soil
319 that was used by the farmer to fill the gully.
320

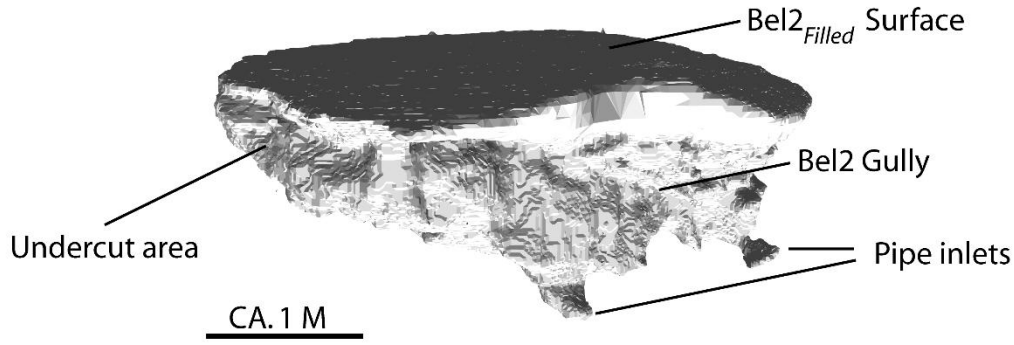

321
322 **Figure 7**: Merged Bel2 and $Bel2_{Filled}$ models for 3D volume calculation showing pipe inlets and
323 undercut gully walls.
324

CITE AS *Frankl, A., Stal, C., Abraha, A., Nyssen, J., Rieke-Zapp, D., De Wulf, A., Poesen, J., 2015. Detailed recording of gully morphology in 3D through image-based modelling. Catena 127, 92-101.*

4. Discussion: Application of image-based 3D modelling in earth sciences

Photo cameras are fairly easy to use and to transport, and therefore, photogrammetric approaches for studying geomorphological processes in the field have been applied since more than 30 years (Welch *et al.*, 1984; Chandler, 1999). Initially, terrestrial photographs were processed in a similar way to aerial photographs, by respecting the schematic block configuration of data acquisition from a vertical perspective. Practically, this was often achieved by mounting one or multiple cameras on a horizontal bar at ca. 2-3 m above the soil surface (Brasington and Smart, 2003). Accuracies provided by these methods proved to be at millimeter level (Rieke-Zapp and Nearing, 2005; Carbonneau *et al.*, 2003). Methodologies and setup of close-range photogrammetric methodologies however often remained complex, time-consuming and expensive (although more cost- and user-friendly methods were also proposed;, Carbonneau *et al.*, 2003) .

Image-based modelling allows to produce accurate 3D models from multiple photographs, in a more flexible, versatile and user-friendly way. As data collection is straightforward and not complex, image-based modelling is rapidly gaining interest of earth scientists, who apply the method at various spatial scales from centimeter to kilometre level. Examples include small rock fragments, stream beds, lava flows, coastal cliffs, moraines, bedrock ridges and volcanic domes (Diefenbach *et al.*, 2012; James and Robson, 2012; Westoby *et al.*, 2012; Bouratsis *et al.*, 2013). Degrees of accuracy are related to the distance between the photographer and the surveyed landform, and is thus dependent on the scale of the latter. In the reported examples, meter to decimeter-level accuracies were achieved for large landforms photographed from air planes or nearby mountain slope (e.g. moraines), while an accuracy at millimetre-level could be achieved

for small objects photographed in a laboratory (rock fragment). This means that, for large landforms, the SfM-MVS approach yields accuracies which are similar to those provided by large-scale aerial photographs, while for smaller features, the method is equivalent to terrain modelling by (terrestrial) LiDAR or laser scanning. As indicated by Diefenbach *et al.* (2012), image-based 3D modelling allows to monitor closely landforms and landscapes at good spatial resolution and at time-intervals appropriate to the study.

For monitoring gully erosion, this study demonstrates that detailed information on gully morphology and volume can be obtained by the use of 3D photomodelling. Novel is that the quantification of gully morphologies is based on the actual 3D morphology, and not on a simplified one that does not include undercut gully walls or pipe inlets. Taking into account the latter is, however, important for assessing the dynamics of the gully and for detailed understanding of gully morphology and processes involved. Gullies which are eroding basically develop through widening and deepening of the channel or by the upslope advance of the headcut (Knighton, 1998). By producing time-series of DEMs erosion rates can be computed, yielding detailed information on the morphologic changes occurring, and thus, on the gully development processes involved. This has already been demonstrated from 2.5D approaches (D'Oleire-Oltmanns *et al*., 2012). The main disadvantage here is, however, that the gully needs to be surveyed over a certain period of time before erosional dynamics can be defined (usually over a rainfall season that accounts for most of the geomorphic change). DEMs produced in a 3D environment can partially add to such interpretations, as they allow to predict much of the change that will occur over time from a single survey. Overhanging walls and soil pipes are

367 geomophologically very unstable an cannot stabilize as such. Mapping the zones in a gully
368 where overhanging walls and piping occurs (by subtracting a 3D model with a 2.5D version of it)
369 therefore yields much information on the gully erosion dynamics which occur, and thus also on
370 the erosion rates to expect. This is especially true for gullies that have accomplished most of their
371 bed degradation and mainly develop through widening. Next to this study, research on the use of
372 SfM-MVS methodologies in gully erosion studies is rapidly increasing, with examples in both
373 2.5D and 3D environments (Castillo *et al.*, 2012; D'Oleire-Oltmanns *et al*., 2012; Kluibenschädl
374 *et al.*, 2013; Kaiser *et al*., 2014).
375 Scanned analogue photographs can also be used in the SfM-MVS methodology, if the metadata
376 normally included in the EXIF-files attached to digital photography are available. Metadata
377 requirements are the focal length, focal point, pixels in X and Y (determines the crop factor) and
378 the pixel size. In the absence of these data, PhotoScan might still be able to create a sparse point
379 cloud, although accuracies are expected to be low (see Agisoft manual at
380 http//:downloads.agisoft.ru). Thus, historical photographs taken from different positions over the
381 same scene can also be used to create 3D models of surface morphologies. Extensive datasets of
382 historical photographs are often available, especially along historical tracks or when considering
383 scenic landscapes (Nyssen *et al.*, 2010). Several studies have demonstrated the value of such
384 datasets in studying landscape features (including gullies) in a semi-quantitative way (e.g. Frankl
385 *et al.*, 2011; Nyssen *et al.*, 2013), and thus image-based 3D modelling offers a new tool to better
386 understand past geomorphic process rates.
387

CITE AS *Frankl, A., Stal, C., Abraha, A., Nyssen, J., Rieke-Zapp, D., De Wulf, A., Poesen, J., 2015. Detailed recording of gully morphology in 3D through image-based modelling. Catena 127, 92-101.*

5. Conclusions

Image-based 3D modelling of gullies is a rather innovative method that allows to rapidly obtain accurate (mm to cm-level) data on gully morphologies and dynamics. Data acquisition is fairly easy and does not require specific equipment besides a photo camera, PhotoScan software (or other existing softwares) and a computer laboratory. The production of 3D models is based on a Structure from Motion-Multi View Stereo (SfM-MVS) workflow. As data-acquisition from the ground perspective allows the integration of undercut gully walls and pipe inlets, image-based modelling provides a tool to quantify the actual 3D morphology of gullies. With that, gully erosion dynamics can be better understood as unstable areas can be detected. This contrasts with approaches using 2.5D models, as can be obtained by aerial photography. For the latter, the gully morphology is simplified due to the limitation of having only one z coordinate per xy set. The flexibility of the method makes it applicable in different environments for which other acquisition methods (e.g., Terrestrial Laser Scanning) are not available, and is suitable when high temporal resolutions are needed in monitoring projects.

Acknowledgements

This research was partially funded with a VLIR-UOS (K219012N) travel grant of Amaury Frankl (Flanders, Belgium). Thanks are also expressed to Gebrekidan Mesfin for field assistance and to the VLIR-UOS team at Mekelle University for logistical support.

References

CITE AS *Frankl, A., Stal, C., Abraha, A., Nyssen, J., Rieke-Zapp, D., De Wulf, A., Poesen, J., 2015. Detailed recording of gully morphology in 3D through image-based modelling. Catena 127, 92-101.*

AGIV, 2008. Uitvoeren van GPS-metingen met behulp van Flemish Positioning Service (FLEPOS). www.agiv.be/flepos, 34.

Alexandre, J., Erpicum, M., Mabille, G., Cornet, Y., 1998. Précipitations atmosphériques et altitude. Prélude à une cartographie des montants annuel et mensuels en Belgique Publications de l'Association Internationale de Climatologie. 11, 219-226.

Bouratsis, P., Diplas, P., Dancey, C.L., Apsilidis, N., 2013. High-resolution 3-D monitoring of evolving sediment beds. Water Resources Research. 49(2), 977-992.

Brasington, J., Smart, R.M.A., 2003. Close range digital photogrammetric analysis of experimental drainage basin evolution. Earth Surface Processes and Landforms. 28(3), 231-247.

Carbonneau, P.E., Lane, S.N., Bergeron, N.E., 2003. Cost-effective non-metric close-range digital photogrammetry and its application to a study of coarse gravel river beds. International Journal of Remote Sensing. 24(14), 2837-2854.

Castillo, C., Pérez, R., James, M.R., Quinton, J.N., Taguas, E.V., Gómez, J.A., 2012. Comparing the Accuracy of Several Field Methods for Measuring Gully Erosion. Soil Science Society of America Journal. 76(4), 1319-1332.

Chandler, J., 1999. Effective application of automated digital photogrammetry for geomorphological research. Earth Surface Processes and Landforms. 24(1), 51-63.

Clarke, M.A., Walsh, R.P.D., 2006. Long-term erosion and surface roughness change of rain-forest terrain following selective logging, Danum Valley, Sabah, Malaysia. Catena. 68(2-3), 109-123.

CITE AS *Frankl, A., Stal, C., Abraha, A., Nyssen, J., Rieke-Zapp, D., De Wulf, A., Poesen, J., 2015. Detailed recording of gully morphology in 3D through image-based modelling. Catena 127, 92-101.*

Corbane, C., Raclot, D., Jacob, F., Albergel, J., Andrieux, P., 2008. Remote sensing of soil surface characteristics from a multiscale classification approach. Catena. 75(3), 308-318.

Diefenbach, A.K., Crider, J.G., Schilling, S.P., Dzurisin, D., 2012. Rapid, low-cost photogrammetry to monitor volcanic eruptions: an example from Mount St. Helens, Washington, USA. Bulletin of Volcanology. 74(2), 579-587.

D'Oleire-Oltmanns, S., Marzolff, I., Peter, K., Ries, J., 2012. Unmanned Aerial Vehicle (UAV) for monitoring soil erosion in morocco. Remote Sensing. 4, 3390–3416.

Frankl, A., Nyssen, J., De Dapper, M., Mitiku Haile, Billi, P., Munro, R.N., Deckers, J., Poesen, J., 2011. Linking long-term gully and river channel dynamics to environmental change using repeat photography (North Ethiopia). Geomorphology. 129(3-4), 238-251.

Frankl, A., Poesen, J., Deckers, J., Haile, M., Nyssen, J., 2012. Gully head retreat rates in the semi-arid highlands of Northern Ethiopia. Geomorphology. 173-174(0), 185-195.

Giménez, R., Marzolff, I., Campo, M.A., Seeger, M., Ries, J.B., Casalí, J., Álvarez-Mozos, J., 2009. Accuracy of high-resolution photogrammetric measurements of gullies with contrasting morphology. Earth Surface Processes and Landforms. 34(14), 1915-1926.

Gómez-Gutiérrez, Á., Schnabel, S., Berenguer-Sempere, F., Lavado-Contador, F., Rubio-Delgado, J., 2014. Using 3D photo-reconstruction methods to estimate gully headcut erosion. Catena. 120, 91-101.

Hendrickx, M., Gheyle, W., Bonne, J., Bourgeois, J., De Wulf, A., Goossens, R., 2011. The use of stereoscopic images taken from a microdrone for the documentation of heritage - An example from the Tuekta burial mounds in the Russian Altay. Journal of Archaeological

Science. 38(11), 2968-2978.

Heritage, G., Hetherington, D., 2007. Towards a protocol for laser scanning in fluvial geomorphology. Earth Surface Processes and Landforms. 32(1), 66-74.

Hülksen, F., Eckes, C., Kuck, R., Unterberg, J., Jörg, S., 2007. Modeling and animating virtual humans for real-time applications. International Journal of Virtual Reality. 6(4), 11-20.

Jacob, M., Frankl, A., Mitiku, H., Zwertvaegher, A., Nyssen, J., 2013. Assessing spatio-temporal rainfall variability in a tropical mountain area (Ethiopia) using NOAA's rainfall estimates, International Journal of Remote Sensing. 34(23), 8305-8321.

James, M.R., Robson, S., 2012. Straightforward reconstruction of 3D surfaces and topography with a camera: Accuracy and geoscience application. Journal of Geophysical Research-Earth Surface. 117, 1-17.

Javernick, L., Brasington, J., Caruso, B., 2014. Modeling the topography of shallow braided rivers using Structure-from-Motion photogrammetry. Geomorphology. 213, 166–182.

Kaiser, A., Neugirg, F., Rock, G., Müller, C., Haas, F., Ries, J., Schmidt, J., 2014. Small-Scale Surface Reconstruction and Volume Calculation of Soil Erosion in Complex Moroccan Gully Morphology Using Structure from Motion. Remote Sensing. 6, 7050-7080.

Kluibenschädl, F., Strohmeier, S., Klik, A., 2013. Assessment of gully erosion by linking photogrammetric methods and field measurements, EGU Geophysical Research Abstracts 5557-4.

Knighton, D., 1998. Fluvial forms and processes - a new perspective. Hodder Education, London.

Lourakis, M., Argyros, A., 2009. SBA: A software package for generic sparse bundle adjustment.

CITE AS *Frankl, A., Stal, C., Abraha, A., Nyssen, J., Rieke-Zapp, D., De Wulf, A., Poesen, J., 2015. Detailed recording of gully morphology in 3D through image-based modelling. Catena 127, 92-101.*

ACM Transactions on Mathematical Software. 36(1), 1-30.

Lucieer, A., de Jong, S., Turner, D., 2013. Mapping landslide displacements using Structure from Motion (SfM) and image correlation of multi-temporal UAV photography. Progress in Physical Geography. DOI: 10.1177/0309133313515293.

Marzolff, I. & Poesen, J. 2009. The potential of 3D gully monitoring with GIS using high-resolution aerial photography and a digital photogrammetry system. Geomorphology 111:48-60.

Merla, G., Abbate, E., Azzaroli, A., Bruni, P., Canuti, P., Fazzuoli, M., Sagri, M., Tacconi, P., 1979. A geological map of Ethiopia and Somalia (1973) 1:2.000.000 and comment. University of Florence, Firenze, Italy.

Montanarella, L., Vargas, R., 2012. Global governance of soil resources as a necessary condition for sustainable development. Current Opinion in Environmental Sustainability. 4(5), 559-564.

Nyssen, J., den Branden, J.V., Spalević, V., Frankl, A., Van de velde, L., Čurović, M., Billi, P., 2013. Twentieth century land resilience in Montenegro and consequent hydrological response. Land Degradation & Development. online early view.

Nyssen, J., Frankl, A., Munro, R.N., Billi, P., Mitiku Haile, 2010. Digital Photographic Archives for Environmental and Historical Studies: An Example from Ethiopia. Scottish Geographical Journal. 126(3). 185 - 207.

Nyssen, J., Naudts, J., De Geyndt, K., Mitiku Haile, Poesen, J., Moeyersons, J., Deckers, J., 2008. Soils and land use in the Tigray highlands (Northern Ethiopia). Land Degradation &

493 Development. 19(3). 257-274.
494 Peel, M.C., Finlayson, B.L., McMahon, T.A., 2007. Updated world map of the Koppen-Geiger
495 climate classification. Hydrology and Earth System Sciences. 11(5), 1633-1644.
496 Perroy, R.L., Bookhagen, B., Asner, G.P., Chadwick, O.A., 2010. Comparison of gully erosion
497 estimates using airborne and ground-based LiDAR on Santa Cruz Island, California.
498 Geomorphology. 118(3-4), 288-300.
499 Perroy, R.L., Bookhagen, B., Chadwick, O.A., Howarth, J.T., 2012. Holocene and Anthropocene
500 Landscape Change: Arroyo Formation on Santa Cruz Island, California. Annals of the
501 Association of American Geographers. 102(6), 1229-1250.
502 Peter, D.K., d'Oleire-Oltmanns, S., Ries, J.B., Marzolff, I., Ait Hssaine, A., 2014. Soil erosion in
503 gully catchments affected by land-levelling measures in the Souss Basin, Morocco,
504 analysed by rainfall simulation and UAV remote sensing data. *Catena*, 113, 24-40.
505 Pfeifer, N., 2002. 3D Terrain models on the basis of a triangulation. Geowissenschaftlichte
506 mitteilungen, 65. Institut für Photogrammetie und Fernkundung, Vienna, Austria.
507 Poesen, J., Govers, G., 1990. Gully erosion in the loam belt of Belgium : typology and control
508 measures. In: Boardman, J., Foster, D, Dearing, J. (Eds.), Soil Erosion on Agricultural
509 Land. Wiley, Chichester, U.K., 513-530.
510 Poesen, J., Nachtergaele, J., Verstraeten, G., Valentin, C., 2003. Gully erosion and environmental
511 change: importance and research needs. Catena. 50(2-4), 91-133.
512 Poesen, J., Vandaele, K. and van Wesemael, B. 1996. Contribution of gully erosion to sediment
513 production in cultivated lands and rangelands. IAHS Publ. 236:251-266.

CITE AS *Frankl, A., Stal, C., Abraha, A., Nyssen, J., Rieke-Zapp, D., De Wulf, A., Poesen, J., 2015. Detailed recording of gully morphology in 3D through image-based modelling. Catena 127, 92-101.*

514 Pollefeys, M., Koch, R., Vergauwen, M., Van Gool, L., 2000. Automated reconstruction of 3D
515 scenes from sequences of images. ISPRS Journal of Photogrammetry and Remote
516 Sensing. 55(4). 251-267.
517 Remondino, F., El-Hakim, S., 2006. Image-based 3D Modelling: A Review. The
518 Photogrammetric Record. 21(115), 269-291.
519 Rieke-Zapp, D.H., Nearing, M.A., 2005. Digital close range photogrammetry for measurement
520 of soil erosion. The Photogrammetric Record, 20(109), 69-87.
521 Ries, J.B., Marzolff, I., 2003. Monitoring of gully erosion in the Central Ebro Basin by large-
522 scale aerial photography taken from a remotely controlled blimp. Catena. 50(2-4), 309-
523 328.
524 Robertson, D., Cipolla, R., 2009. Structure from motion. In: Varga, M. (Ed.), Practical image
525 processing and computer vision. John Wiley, Hoboken, NJ, USA., 49.
526 Schumm, S.A., 2005. River variability and complexity. Cambridge University Press, New York.
527 Seitz, S., Curless, B., Diebel, J., Scharstein, D., Szeliski, R., 2006. A comparison and evaluation
528 of multi-view stereo reconstruction algorithms, IEEE Computer Society Conference on
529 Computer Vision and Pattern Recognition, New York, NY, USA, 17-22 June, 519-528.
530 Stal, C., De Wulf, A., De Coene, K., De Maeyer, P., Nuttens, T., Ongena, T., 2012. Digital
531 Representation of Historical Globes: Methods to Make 3D and Pseudo-3D Models of
532 Sixteenth Century Mercator Globes. The Cartographic Journal. 49(2), 107-117.
533 Stal, C., De Wulf, A., Nuttens, T., De Maeyer, P., Goossens, R., 2011. Reconstruction of a
534 medieval wall: photogammetric mapping and quality analysis by terrestrial laser scanning.

CITE AS *Frankl, A., Stal, C., Abraha, A., Nyssen, J., Rieke-Zapp, D., De Wulf, A., Poesen, J., 2015. Detailed recording of gully morphology in 3D through image-based modelling. Catena 127, 92-101.*

31th EARSeL symposium : Remote sensing and geoinformation not only for scientific cooperation, Prague, Czech Republic, 54-65.

Valentin, C., Poesen, J., Li, Y., 2005. Gully erosion: Impacts, factors and control. Catena. 63(2-3), 132-153.

Vanwalleghem, T., Poesen, J., Nachtergaele, J., Verstraeten, G., 2005. Characteristics, controlling factors and importance of deep gullies under cropland on loess-derived soils. Geomorphology. 69(1-4), 76-91.

Verhoeven, G., Doneus, M., Briese, C., Vermeulen, F., 2012. Mapping by matching: a computer vision-based approach to fast and accurate georeferencing of archaeological aerial photographs. Journal of Archaeological Science. 39(7), 2060-2070.

Welch, R., Jordan, T., Thomas, A.W., 1984. A photogrammetric technique for measuring soil erosion. Journal of Soil and Water Conservation. 39(3), 191-194.

Westoby, M.J., Brasington, J., Glasser, N.F., Hambrey, M.J., Reynolds, J.M., 2012. "Structure-from-Motion" photogrammetry: A low-cost, effective tool for geoscience applications. Geomorphology. 179(0), 300-314.